Developmental Cell
Article

p63 Mediates an Apoptotic Response to Pharmacological and Disease-Related ER Stress in the Developing Epidermis

Ujwal J. Pyati,[1] Evisa Gjini,[1,*] Seth Carbonneau,[1] Jeong-Soo Lee,[1] Feng Guo,[1] Cicely A. Jette,[2] David P. Kelsell,[3] and A. Thomas Look[1,*]
[1]Department of Pediatric Oncology, Dana-Farber Cancer Institute and Harvard Medical School, 44 Binney Street, Boston, MA 02115, USA
[2]Department of Oncological Sciences, Huntsman Cancer Institute, 2000 Circle of Hope, Salt Lake City, UT 84112, USA
[3]Centre for Cutaneous Research, Institute of Cell and Molecular Science, Barts and The London School of Medicine and Dentistry, Queen Mary University of London, 4 Newark Street, London E1 2AT, UK
*Correspondence: evisa_gjini@dfci.harvard.edu (E.G.), thomas_look@dfci.harvard.edu (A.T.L.)
DOI 10.1016/j.devcel.2011.07.012

SUMMARY

Endoplasmic reticulum (ER) stress triggers tissue-specific responses that culminate in either cellular adaptation or apoptosis, but the genetic networks distinguishing these responses are not well understood. Here we demonstrate that ER stress induced in the developing zebrafish causes rapid apoptosis in the brain, spinal cord, tail epidermis, lens, and epiphysis. Focusing on the tail epidermis, we uncover an apoptotic response that depends on Puma, but not on p53 or Chop. *puma* is transcriptionally activated during this ER stress response in a p53-independent manner, and is an essential mediator of epidermal apoptosis. We demonstrate that the p63 transcription factor is upregulated to initiate this apoptotic pathway and directly activates *puma* transcription in response to ER stress. We also show that a mutation of human Connexin 31, which causes erythrokeratoderma variabilis, induces ER stress and p63-dependent epidermal apoptosis in the zebrafish embryo, thus implicating this pathway in the pathogenesis of inherited disease.

INTRODUCTION

In all eukaryotic cells, the endoplasmic reticulum (ER) serves the critical cellular functions of protein translation, calcium storage, and folding and processing of membrane and secreted proteins (Rao et al., 2004). When the load of proteins to be folded in the ER exceeds the capacity of cellular chaperones to aid in the folding process, a response known as the ER stress pathway, or unfolded protein response (UPR; reviewed in Malhotra and Kaufman, 2007; Ron and Walter, 2007), is triggered. Shortly after the onset of ER stress, cells activate three proximal pathways, mediated by IRE1, ATF6, and PERK, to upregulate the transcription and translation of ER chaperones, amino acid biosynthesis enzymes, and the endoplasmic reticulum-associated degradation (ERAD) proteins. Successful engagement of these pathways can lower the unfolded protein load and return the cell to homeostasis. However, severe or prolonged stress can lead to an apoptotic response (Fribley et al., 2009), and the cellular outcome is central to a variety of human diseases including cancer, inherited skin disorders, diabetes, and neurodegenerative disorders (Lin et al., 2008; Tattersall et al., 2009). The tissue-specific decisions responsible for apoptotic outcomes in diseased and normal cells are still poorly understood, warranting further research into how distinct vertebrate tissues integrate molecular signaling downstream of the proximal ER stress pathways to determine whether cells initiate programmed cell death or overcome the stress response and survive.

While the decisive events that induce cellular apoptosis after ER stress are not fully understood, the signaling pathways that sense and respond to ER stress have been extensively studied. Seminal work to elucidate these proximal ER stress pathways in yeast led to the discovery that the trans-ER membrane-bound IRE1 (inositol requiring enzyme-1) protein contains both kinase and endoribonuclease activities, which are triggered after stress in the ER (Cox et al., 1993; Mori et al., 1993). When the load of unfolded proteins in the ER lumen becomes excessive, the protein-folding chaperone BiP (Hspa5) detaches from IRE1 (Bertolotti et al., 2000; Okamura et al., 2000), resulting in *trans*-autophosphorylation of the IRE1 homodimer, which activates the endoribonuclease activity of IRE1 and the subsequent unconventional splicing of *HAC1* mRNA (Sidrauski and Walter, 1997). This unconventional splicing alters the reading frame for translation of the HAC1 protein, resulting in the synthesis of a highly active transcription factor that can activate a wide array of downstream target genes, including those encoding protein chaperones and others encoding the ERAD components (Kopito, 1997; Travers et al., 2000). This work established the IRE1-HAC1 pathway as the most ancient and most conserved proximal ER stress pathway in eukaryotes.

Two additional ER stress pathways have been delineated in multicellular organisms (Ron and Walter, 2007). The ATF6 protein, a trans-ER membrane molecule, is directed to the Golgi apparatus upon activation via BiP uncoupling, where it undergoes cleavage by Site-1 and Site-2 proteases to become an active transcription factor (Haze et al., 1999). Like XBP1 (the target of mammalian IRE1), ATF6 can activate the transcription of a myriad of recovery genes to allow the stressed cell to repair

its ER burden and survive. It also induces the transcription of XBP1, providing a cross-talk mechanism between the ATF6- and IRE1-mediated ER stress pathways (Yoshida et al., 2001). The third ER stress pathway directly triggers global translational attenuation to lessen the rate of unfolded proteins accumulating in the ER. When released by BiP, the trans-ER protein PKR-like endoplasmic reticulum kinase (PERK), directly phosphorylates eukaryotic translation initiation factor 2α (eIF2α) (Harding et al., 1999). This phosphorylation on serine 51 greatly diminishes the ability of eIF2α to initiate the cap-dependent translation of cellular proteins, thus reducing the overall amount of proteins in the ER. Remarkably, however, mRNA encoding the transcription factor ATF4 is preferentially translated due to the presence of small upstream ORFs (uORFs), resulting in a paradoxical upregulation of translation of this gene in response to phosphorylation of eIF2α (Harding et al., 2000). ATF4 then enters the nucleus as an active transcription factor that initiates the transcription of downstream target genes, including the pro-apoptotic transcription factor Chop. While no Chop homolog exists in worms, mammalian Chop contributes to some forms of ER stress-induced apoptosis and can kill cells when overexpressed (Matsumoto et al., 1996; Maytin et al., 2001; Zinszner et al., 1998).

Although work in yeast, worms, mice, and human cell culture has provided valuable insights into the proximal mechanisms that cells and tissues use to cope with ER stress, many of the downstream molecular events that determine stress-induced outcomes remain elusive. Here, we take advantage of the rapid chemical uptake properties of the zebrafish embryo to analyze the timing and spatial activation of ER stress, together with its apoptotic consequences, after the whole-animal application of thapsigargin or brefeldin A, two well-characterized ER stress-inducing compounds. In developing embryos treated with either drug, we demonstrate that cells within the lens, epiphysis, and tail epidermis undergo ER stress-induced apoptosis within 4 hr in a p53-independent manner. Further, we show that this rapid apoptotic response requires the BH3-only gene *puma*. Using morpholino knockdown, we demonstrate that the transcription factor p63 is required for *puma* expression, and further that p63 directly binds the *puma* promoter in vivo following an increase in p63 levels. Finally, we demonstrate that p63 mediates an in vivo apoptotic response to mutant Connexin 31, a protein produced as a result of a dominantly inherited mutation in humans that induces an ER stress response in the epidermis of the skin, contributing to the disease erythrokeratoderma variabilis (EKV).

RESULTS

ER Stressors Induce p53-Independent Apoptosis in the Brain, Spinal Cord, Lens, Epiphysis, and Tail Epidermis of Early Zebrafish Embryos

To test whether zebrafish undergo ER stress-induced apoptosis in vivo, we first treated 24 hr postfertilization (hpf) embryos with thapsigargin, a potent ER calcium pump inhibitor that induces ER stress in mammalian cells (Pahl and Baeuerle, 1995). This treatment interval was chosen because most major developmental patterning is complete at this stage, allowing the assessment of tissue-specific cell death (Pyati et al., 2007). After 4 hr of continuous treatment with thapsigargin, we observed focal increases in apoptotic cell death as assayed by whole-mount TUNEL staining (Figures 1A–1F) (Jette et al., 2008). Increased TUNEL positivity was evident in the brain, spinal cord, lenses of the eyes, epiphysis (which ultimately forms the pineal gland), and tail epidermis (Figure 1). TUNEL staining was most pronounced in the latter three tissues, with less positivity in the brain and spinal cord. These data show that specific tissues within developing embryos are sensitive to thapsigargin-induced ER stress and rapidly undergo apoptosis.

In mammals, ER stress-induced apoptosis can be triggered in either a p53-dependent or -independent manner, depending on the context (Galehdar et al., 2010; Puthalakath et al., 2007; Reimertz et al., 2003). To test whether p53 is required for ER stress-induced apoptosis in the zebrafish, we treated embryos that carry a homozygous inactivating mutation within the DNA-binding domain of *p53* (*p53*$^{e7/e7}$; Berghmans et al., 2005; Sidi et al., 2008) with thapsigargin. As in wild-type embryos, we observed a marked increase in apoptotic cells by TUNEL staining (Figures 1G–1L) in *p53* mutants. To confirm that the observed tissue-specific apoptosis was due to ER stress, we treated embryos with brefeldin A, which disrupts ER to Golgi trafficking of membrane and secreted proteins (Samali et al., 2010). Similar to thapsigargin, brefeldin A triggered a p53-independent apoptotic response that was most prominent in the lens, epiphysis, and tail epidermis after 4 hr of treatment (Figures 1M–1R). Since thapsigargin treatment caused a more robust cell death response than did brefeldin A after 4 hr (compare Figures 1J–1L and 1P–1R), we chose to use thapsigargin for most subsequent experiments, reserving brefeldin A to confirm key results. Taken together, these data show that ER stress-inducing drugs trigger apoptosis in zebrafish embryos independently of p53.

To determine the spatial extent of ER stress induced by thapsigargin, we examined expression of the ER stress recovery gene *bip* by whole-mount in situ hybridization (Figures 1S–1V). Similar to reports for mammalian cells, we observed a robust posttreatment increase of *bip* that was especially prominent in the tail epidermis, lens, and epiphysis, where we had observed apoptosis in our whole-mount TUNEL assays. Interestingly, we also observed increased *bip* expression in many parts of the head as well as in the hatching gland, where we saw lower levels of apoptosis. Similar staining was observed following brefeldin A treatment, confirming the selective sensitivity of distinct embryonic tissues to ER stressors (Figure S1 available online). Since the most robust apoptotic response to ER stress occurred in the tail epidermis (Figures 1F, 1L, and 1R), we cryosectioned thapsigargin-treated embryos followed by TUNEL staining, to determine the precise tissue layer(s) that underwent cell death in this region. As shown in Figures 1W–E1, the primary location of apoptotic cells in the tails of both *AB* and *p53* mutant embryos was the epidermal cell layer (marked by arrowheads). Thus, ER stress triggers rapid apoptosis in the developing tail that is primarily localized to the epidermis, which later becomes the skin of the zebrafish.

ER Stress Activates Proximal UPR Pathways within 1 Hr in Zebrafish Embryos

To asses the kinetics of ER stress-induced apoptosis in zebrafish embryos, we examined thapsigargin-treated embryos by

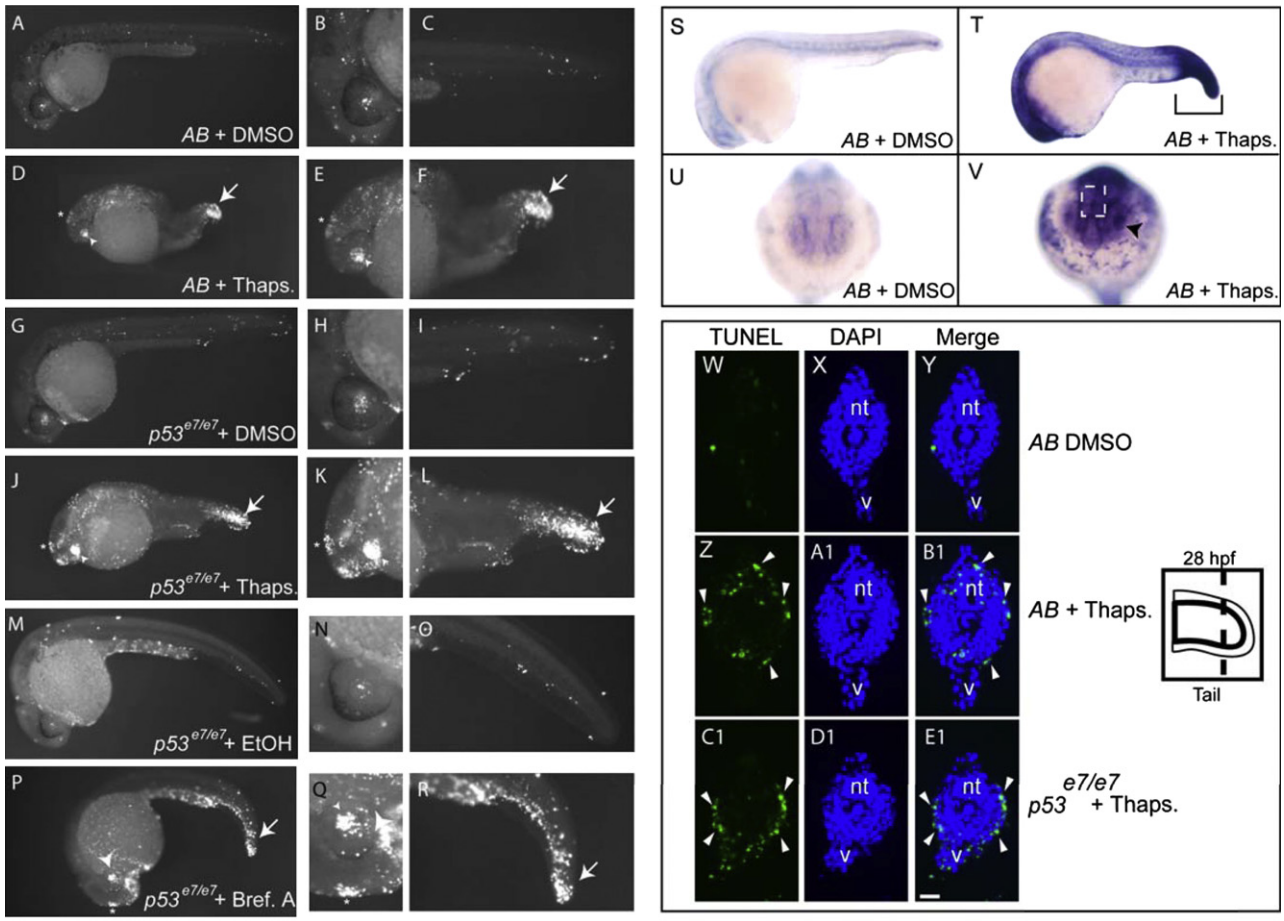

Figure 1. ER Stressors Trigger *bip* Upregulation and Apoptosis in the Lens, Epiphysis, and Tail Epidermis of 24 Hpf Zebrafish Embryos

Embryos (24 hpf) from an *AB* incross or a stage-matched *p53* homozygous mutant incross were treated with a DMSO vehicle or 5 μM thapsigargin for 4 hr, fixed, and assayed for apoptosis by TUNEL labeling.

(A–C) Scattered cells in *AB* DMSO-treated control embryos (n = 29) showed TUNEL positivity.

(D–F) Thapsigargin-treated *AB* embryos had increased TUNEL positivity that was concentrated in the epiphysis, lens, and tail (93% of embryos with increased apoptosis, n = 30).

(G–I) *p53* homozygous mutant embryos treated with DMSO (n = 31) showed comparable levels of TUNEL positivity to *AB* DMSO-treated embryos.

(J–E1) *p53* homozygous mutant embryos treated with thapsigargin showed increased apoptosis in the same regions as in *AB* embryos (100% of embryos with increased apoptosis, n = 31). Like thapsigargin treatment, Brefeldin A treatment (5 ug/ml) caused increased apoptosis in the lens, epiphysis, and tail (P–R) compared to vehicle-treated controls (M–O) (see also Figure S1). Compared to DMSO-treated controls (S and U), *bip* expression was upregulated in embryos treated for 3 hr with thapsigargin (T and V). In cryosections, DMSO controls (W–Y) had minimal apoptosis, while thapsigargin treatment of both AB embryos (Z–B1) and p53 mutant embryos (C1–E1) caused extensive enriched apoptosis in the tail epidermis (white arrowheads).

In (A)–(R), zoomed images of head and tail are shown at the right of corresponding whole-embryo images. Asterisks indicate epiphysis, arrowheads the lens, and arrows the tail in thapsigargin-treated embryos.

TUNEL staining every hour for 4 hr. By 2 hr, we observed an increase in cell death, mainly in the tail, followed by a gradual increase in dying cells within the tail, lens, and epiphysis, until peak levels were reached at 4 hr posttreatment (Figures 2A–2D).

In mammalian cells, ER stressors activate proximal ER stress pathways through three major trans-ER membrane proteins: IRE1, ATF6, and PERK (Malhotra and Kaufman, 2007; Ron and Walter, 2007). In the zebrafish embryo, we interrogated the kinetics of the Ire-1 and Perk pathways, measuring over time the endogenous ER-membrane associated "unconventional" splicing of *xbp-1* (as a direct readout of IRE1 activation; Calfon et al., 2002) and the phosphorylation of eIF2α (as a direct readout of PERK activation; Harding et al., 1999), using cell lysates prepared from pooled thapsigargin-treated embryos. Analysis of *xbp-1* splicing indicated that the Ire-1 pathway was activated after only 45 min of thapsigargin treatment (Figure 2E) and was sustained over 4 hr. Measurements of endogenous levels of phosphorylated eIF2α indicated that Perk was activated after 1 hr of treatment and was continuously activated for 4 hr (Figure 2F). Thus, thapsigargin-treated zebrafish embryos rapidly activate proximal ER stress pathways, as indicated by the prompt induction of *xbp-1* splicing by Ire-1 at 45 min posttreatment and by phosphorylation of eIF2α after an additional 15 min.

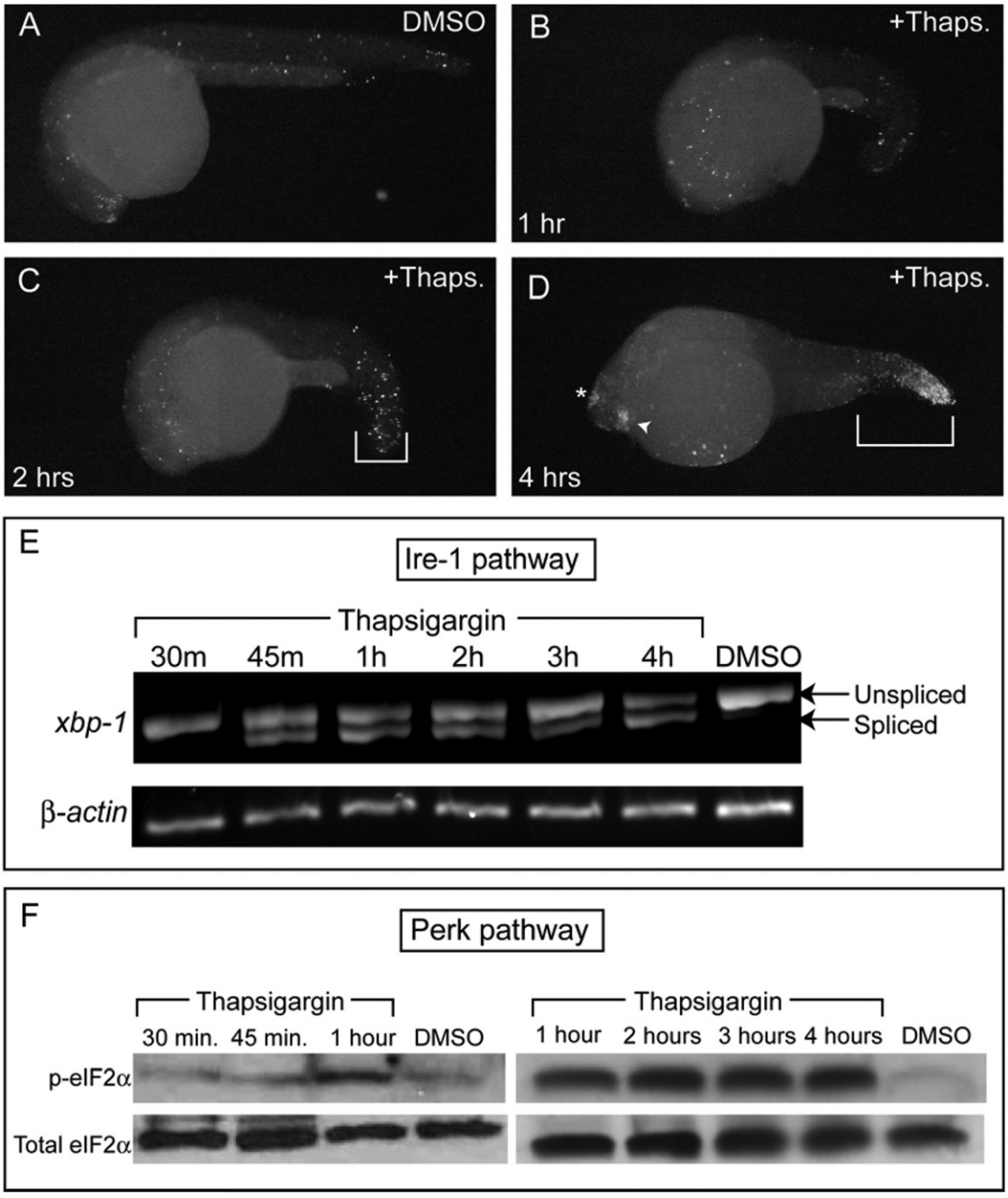

Figure 2. Thapsigargin Treatment Rapidly Activates Conserved Vertebrate ER Stress Pathways to Induce Apoptosis

(A–D) TUNEL staining was performed in fixed embryos after (A) 4 hr of DMSO treatment or after (B) 1 hr, (C) 2 hr, or (D) 4 hr of thapsigargin treatment. (C) Increased apoptosis was first apparent in the tail by 2 hr of thapsigargin treatment, but robust apoptosis in the lens, epiphysis, and tail was evident only after (D) 4 hr of thapsigargin treatment compared to DMSO controls at the same stage. All images are representative of embryos examined at each time point (n = 10 in all treatments except D, where n = 9).

(E) By RT-PCR, *xbp-1* splicing in the Ire-1 pathway was first apparent after 45 min of thapsigargin treatment, and was maintained over 4 hr. Note the lower band present from 45 min on, which corresponds to the nonconventional splice-form downstream of Ire-1 activation.

(F) Antiphospho eIF2α immunoblots showed that eIF2α was robustly phosphorylated in the Perk pathway from 1 hr through the end of the thapsigargin time-course. Total eIF2α was immunoblotted as a loading control after stripping of the original blot.

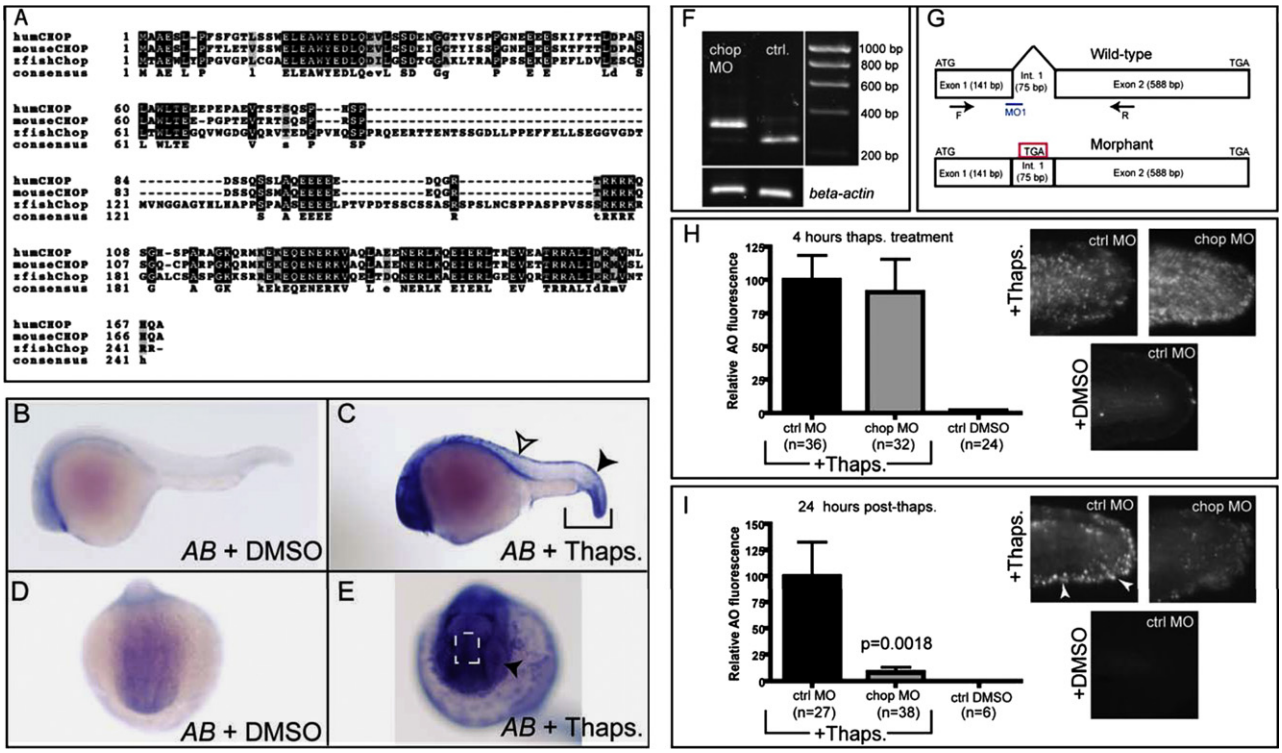

Figure 3. Zebrafish Chop Is Dispensable for Rapid ER Stress-Induced Apoptosis, but Is Required for 24 Hr Apoptosis in the Caudal Fin Fold

(A) Alignment of zebrafish Chop with human and mouse orthologs. Consensus sequence is listed below the aligned sequences.

(B–D) DMSO-treated embryos have minimal chop expression, while embryos treated with thapsigargin for 3 hr (C) have high levels of chop expression in the tail (brackets), including the tail epidermis (black arrowhead). Expression was also observed in the dorsal trunk epidermis (open arrowhead in C).

(E) An anterior view reveals additional chop expression in the epiphysis region (dashed white box) and the lens (black arrowhead). Images in (B)–(E) represent 100% of embryos examined; n $\geq$ 14 embryos per condition.

(F) Agarose gel (1%) showing alternate splice product generated 28 hr after *chop* morpholino (MO) injection compared to uninjected controls (Ctrl.); both groups of embryos were treated with thapsigargin at 24 hpf.

(G) Depiction of splice-blocking event in *chop* morphant mRNA compared to wild-type, as determined by sequencing.

(H) *chop* morpholino (5 ng) was injected into *p53* homozygous mutant embryos, which were then grown to 24 hpf, treated with thapsigargin for 4 hr, and assayed for cell death by AO staining. Cropped photos were quantitated for total fluorescence intensity with Volocity software, and values were normalized to controls.

(I) *chop* morpholino-injected embryos were grown to 24 hpf, treated with thapsigargin for 4 hr, washed into egg medium, left for 24 hr, and then stained with AO and assayed as in (H). All data are represented as means ± SEM.

Chop Is Dispensable for the Rapid ER Stress-Induced Apoptotic Pathway but Is Essential for Late ER Stress-Induced Apoptosis

In mammalian systems, the pro-apoptotic transcription factor Chop is necessary to elicit peak levels of cell death following ER stress induction in some contexts (Zinszner et al., 1998). We thus sought to determine whether the zebrafish genome harbors a *chop* ortholog and whether Chop plays a critical pro-apoptotic role in the zebrafish epidermis as in some mammalian tissues. By performing a BLAST search in the Ensembl genome server using the human CHOP sequence, we identified a single highly similar sequence located on chromosome 5 of the zebrafish genome. This putative ortholog showed a close syntenic relationship to mouse and human CHOP, with coding regions for similar genes in direct proximity (www.ensembl.org). Based on our cloned and verified cDNA fragment for the full-length to Chop coding region, the predicted zebrafish Chop protein, although divergent in length from human and mouse isoforms, shares particularly high sequence identity in the C-terminal DNA-binding domain (brackets in Figure 3A). Thus, we conclude that the zebrafish genome contains a single zebrafish *chop* ortholog that encodes a protein with a highly conserved DNA binding-domain sequence.

Next, we wished to determine whether zebrafish *chop,* like human CHOP, is transcriptionally activated following ER stress. In 24-hpf embryos treated with thapsigargin for 3 hr, we observed robust induction of this pro-apoptotic factor at the end of treatment (Figure 3B–3E). Similar to *bip* (Figure 1), the expression of *chop* was tissue-restricted and enriched in the tail (brackets in Figure 3C), lens (black arrowhead in Figure 3E), and epiphysis region (box in Figure 3E). *Chop* expression was also induced in the dorsal epidermis (white arrowhead in Figure 3C), where we had observed minimal apoptosis in our TUNEL assays (Figure 1). Importantly, brefeldin A triggered *chop* expression in similar tissues and with similar kinetics (Figure S1), confirming that zebrafish *chop* is generally ER stress-responsive and not solely responsive to thapsigargin.

To test whether zebrafish Chop is required in vivo for the ER stress-induced apoptotic pathway in tail epidermis, we injected a *chop*-specific splice-blocking morpholino (Robu et al., 2007)

into *p53* homozygous mutant embryos (to eliminate any nonspecific morpholino toxicity that could confound our results (Figures 3F and 3G). Next, to quantify the level of apoptosis induction, we treated morpholino-injected embryos with thapsigargin for 4 hr starting at 24 hpf and performed AO staining in live embryos to mark dead and dying cells. Remarkably, despite nearly complete knockdown of Chop (Figure 3F), we still observed marked ER stress-induced cell death after 4 hr of thapsigargin treatment (Figure 3H), indicating that this apoptotic pathway was rapidly triggered independently of both Chop and p53.

Multiple studies in mammalian cell culture have shown that Chop deficiency attenuates ER stress-induced apoptosis over a prolonged period (Puthalakath et al., 2007; Zinszner et al., 1998). Thus, we asked whether a delayed ER stress-induced cell death response occurs that is distinct from the rapid apoptotic response shown in Figure 1, and whether it depends on Chop. We injected either a control morpholino or the *chop* morpholino into *p53* mutant embryos, treated 24 hpf embryos with thapsigargin for 4 hr, and then washed out the drug and assayed for cell death by AO staining 24 hr later. Since AO staining provides a transient image of dying cells during development (Abrams et al., 1993), we reasoned that this vital dye would mark only cells that were dying or had died within 24 hr posttreatment. Indeed, control morphants displayed cell death at 24 hr posttreatment that was distinct from the cell death we observed in the 4 hr apoptotic assay (Figure 3I). This cell death was enriched in the caudal fin fold (white arrowheads in Figure 3I), in cells that normally develop into the tail fins (Webb and Kimelman, 2005), with significantly decreased cell death in the lateral region of the tail. In contrast to control morpholino-injected embryos, *chop* morpholino-injected embryos showed very few dying cells in the tail at this stage (Figure 3I). These data are consistent with the expression pattern of *chop* in the caudal fin fold epidermis following ER stress (black arrowhead in Figure 3C), suggesting that developing caudal fin cells die at 24 hr posttreatment in a Chop-dependent manner that does not require *p53*. Importantly, we could block all ER stress-induced cell death by overexpression of mRNA encoding Bcl-2 (Figure S2), confirming that intrinsic mitochondrial apoptosis is induced by ER stress in this system. We conclude that zebrafish embryos activate both a rapid Chop-independent apoptotic pathway within 4 hr of ER stress induction, and a separate Chop-dependent apoptotic pathway 24 hr later. Interestingly, 5-dpf thymocytes were also sensitive to ER stress, indicating that these pathways can still be triggered beyond early development (Figure S3).

puma Is Transcriptionally Activated Following ER Stress and Is Necessary for Rapid Epidermal Apoptosis

To discover which genes are transcriptionally activated and critical for the Chop-independent cell death program, we performed cDNA microarray analysis using dissected tails from pooled thapsigargin-treated embryos in both the *AB* and *p53* mutant backgrounds. By using dissected tail tissue only, we reasoned that we could decrease the influence of developmental gene expression elsewhere in the organism and maximize the fold induction of ER stress-responsive genes in the tail epidermis. Among the list of the 50 most upregulated genes after thapsigargin treatment, there were numerous known mammalian ER stress-induced genes, including *igfbp1a*, *junb*, *dusp2*, *atf3*, *fos*, and *dnajc3*. These results indicate that thapsigargin induces a rapid ER stress response in the zebrafish epidermis similar to that in mammals. Interestingly, when we analyzed the 50 most highly ER stress-activated genes, we discovered that the pro-apoptotic BH3-only gene *puma* was among this group (Figure 4A), showing an ~6-fold upregulation in thapsigargin-treated tails compared to DMSO controls. Since Bcl-2 overexpression could block the early apoptotic pathway (Figure S2), we considered *puma* to be a strong candidate for the pro-apoptotic BH3-only gene that was activated to kill tail epidermal cells. Indeed in thapsigargin-treated embryos, *puma* was induced in many parts of the brain as well as the lens, epiphysis, and tail, where rapid ER stress-induced apoptosis was most robust (Figures 4B and 4C). Furthermore, as observed in the microarrays, the transcriptional activation of *puma* was p53-independent (Figures 4D and 4E), supporting a role for this factor in ER stress-induced apoptosis. Importantly, we observed a similar increase in *puma* transcription following brefeldin A treatment, supporting the hypothesis that *puma* activation is part of the general response to ER stress induction, and not specific to thapsigargin treatment (Figure S3).

To determine whether Puma is critical for epidermal ER stress-induced apoptosis in vivo, we injected a *puma* splice-blocking morpholino (Sidi et al., 2008) into *p53* mutant embryos and treated the embryos with thapsigargin for 4 hr (Figures 4F and 4G). *puma* knockdown strongly blocked the 4 hr apoptotic response in the lateral tail epidermis (Figure 4F), showing that *puma* transcriptional induction is the apoptotic "trigger" downstream of ER stress. This result was confirmed with brefeldin A (Figure S3), indicating that *puma* is required for the apoptotic response to multiple ER stressors. Despite its requirement for the 4 hr Chop-independent apoptotic response, Puma was not required for the 24 hr Chop-dependent apoptotic response (Figure 4G), further demarcating these two pathways. Thus, ER stress activates *puma* expression within 3 hr in the tail epidermis in a Chop and p53-independent manner, while upregulation of *puma* is critical for the subsequent 4 hr apoptotic response in vivo.

p63 Is Required for the Activation of *puma* and Apoptotic Death that Occurs 4 Hr after ER Stress in the Epidermis

Because p63 and p73 partially overlap with p53 in their transcriptional targets (Harms et al., 2004), we could not be certain about the stringency of the requirement for p63 in *puma* activation. Thus, using published morpholinos against both *p63* (Sidi et al., 2008) and *p73* (Rentzsch et al., 2003) (Figure S4). We compared the effects of these knockdowns on *puma* expression in homozygous p53 mutant fish after induction of ER stress. As shown in Figure 5, p63 knockdown, but not p73 knockdown, markedly reduced *puma* activation after 3 hr of thapsigargin treatment in the lens, epiphysis, and tail epidermis (Figure 5B) compared with findings in controls (Figure 5A) or *p73* morphants (Figure 5C). This reduction was especially pronounced in the tail epidermis, where *puma* expression was nearly absent in *p63* morphants.

The above results suggest that knockdown of p63 would likely, given the importance of Puma in this response, block ER stress-induced apoptosis in the epidermis. To test this prediction, we treated *p63* and control morpholino-injected *p53*

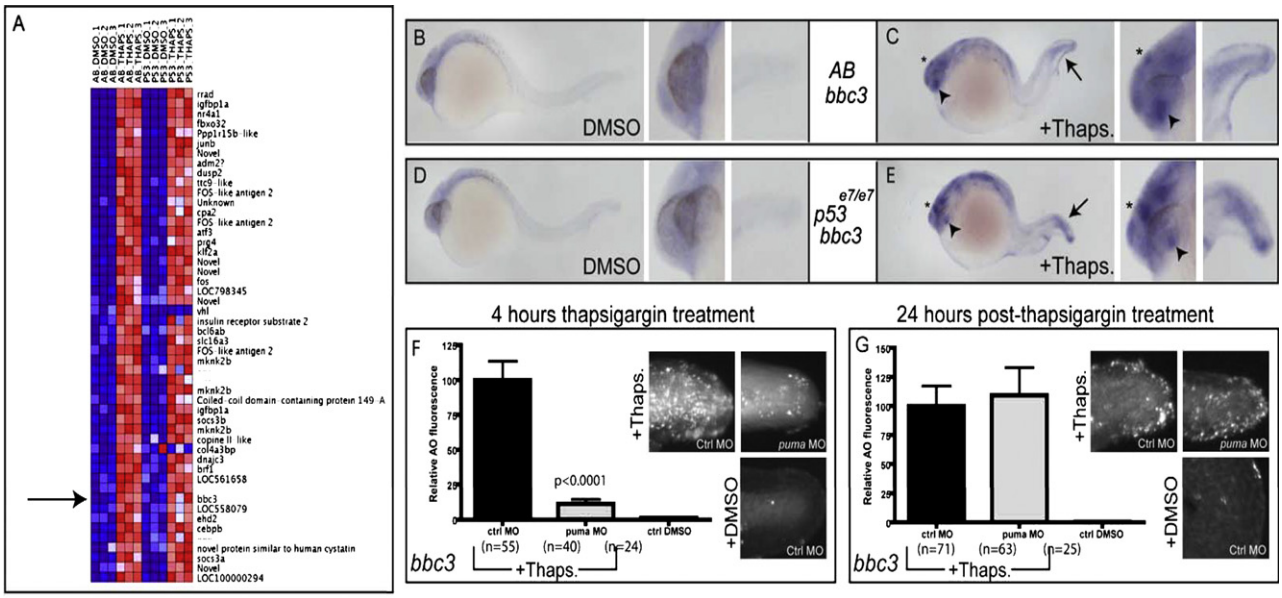

Figure 4. *puma* Expression Is Increased in a p53-Independent Manner Following Thapsigargin Treatment

(A) Microarray analysis of dissected tail tissue revealed increased puma expression following thapsigargin treatment in both *AB* and *p53* mutant embryos. (B–E) Compared to DMSO-treated controls (B), thapsigargin-treated embryos (C) had increased puma expression in the tail (arrow), epiphysis (asterisk), and lens (arrowhead). This increased expression was also observed in thapsigargin-treated *p53* mutant embryos (E) compared to DMSO-treated controls (D). (F and G) Knockdown of *puma* attenuated 4 hr ER stress-induced apoptosis, but not (G) 28 hr ER stress-induced apoptosis. See also Figure S2 and Figure S3.

mutant embryos with thapsigargin at 24 hpf and performed AO staining 4 hr later. Since *p63* and *p73* loss-of-function have been reported to increase apoptosis that is unrelated to ER stress (Pietsch et al., 2008), we also examined DMSO control embryos for each of these morpholino injections. *p63* morphants treated with thapsigargin had markedly decreased AO fluorescence compared to controls treated in the same manner (Figure 5D). Both thapsigargin-treated and DMSO-treated *p63* morphants showed weak AO positivity in the outer fin epidermis at this stage (white arrowheads in Figure 5D), supporting previously described roles for *p63* in fin development (Bakkers et al., 2002; Lee and Kimelman, 2002). However, neither of these conditions with *p63* knockdown displayed the robust AO positivity of control morphants treated with thapsigargin, particularly in the lateral epidermis of the tail (black arrowhead in Figure 5D). Repeated AO staining after brefeldin A treatment yielded similar results (Figure S5), confirming the involvement of p63 in epidermal apoptosis induced by ER stress. By contrast, *p63* knockdown did not block the late Chop-dependent apoptotic pathway (Figure 5E) while *p73* knockdown failed to block either the early or late apoptotic response (Figures 5F and 5G). Importantly, we observed similar results in *AB* embryos (Figure S5), showing that p63 is not simply redundant with p53 in this apoptotic response, but, rather acts independently of p53 to induce apoptosis in epidermal cells following ER stress.

To confirm our *p63* knockdown results with a second apoptotic assay, we performed dual immunofluorescence for activated Caspase-3 to mark apoptotic cells (in green) and for p63 (in red) to indicate the extent of p63 protein deficiency (Figures 5H–5K). Compared to the standard control morpholino, the *p63* splice-blocking morpholino effectively reduced p63 protein levels and eliminated Caspase-3 activation in the lateral epidermis of thapsigargin-treated embryos, confirming that p63 is required for Caspase-3 activation following ER stress.

Unlike mammals, which have six different isoforms of p63 (Yang et al., 1998), the only isoform of p63 thus far detected in zebrafish is ΔNp63α (Bakkers et al., 2002; Lee and Kimelman, 2002). Nonetheless, since our *p63* splice-blocking morpholino could affect all potential isoforms of p63 (Sidi et al., 2008), we repeated our apoptosis assay using a second morpholino designed to block only the translation of *ΔNp63*. As shown in Figure 5J, the *ΔNp63*-specific morpholino blocked 4 hr apoptosis similar to the pan-p63 morpholino, showing that the pro-apoptotic effects of p63 are elicited through ΔNp63.

Finally, to determine the spatial distribution of p63 in the tail epidermis relative to the dying cells observed in the 4 hr apoptotic response, we performed dual confocal immunofluorescence using the p63 antibody together with the activated-Caspase-3 antibody. By examining single optical sections obtained from confocal microscopy, we analyzed clusters of p63-positive cells within the tail epidermis of 28-hpf embryos (schematized by red region in Figure 5L). While DMSO-treated embryos showed minimal activation of Caspase-3 (Figure 5M), embryos treated with thapsigargin for 4 hr showed clear Caspase-3 activation in the tail epidermis (Figure 5N). In other systems, the activated form of Caspase-3 has been shown to translocate from the cytoplasm to the nucleus during apoptosis (Kamada et al., 2005); accordingly, we observed activated Caspase-3 staining that partially overlapped with p63-positive nuclear staining in ~50% of cells within the tail epidermis (see arrowheads in Figure 5N), indicating that apoptosis was occurring in p63-expressing cells. Together, these data show that in

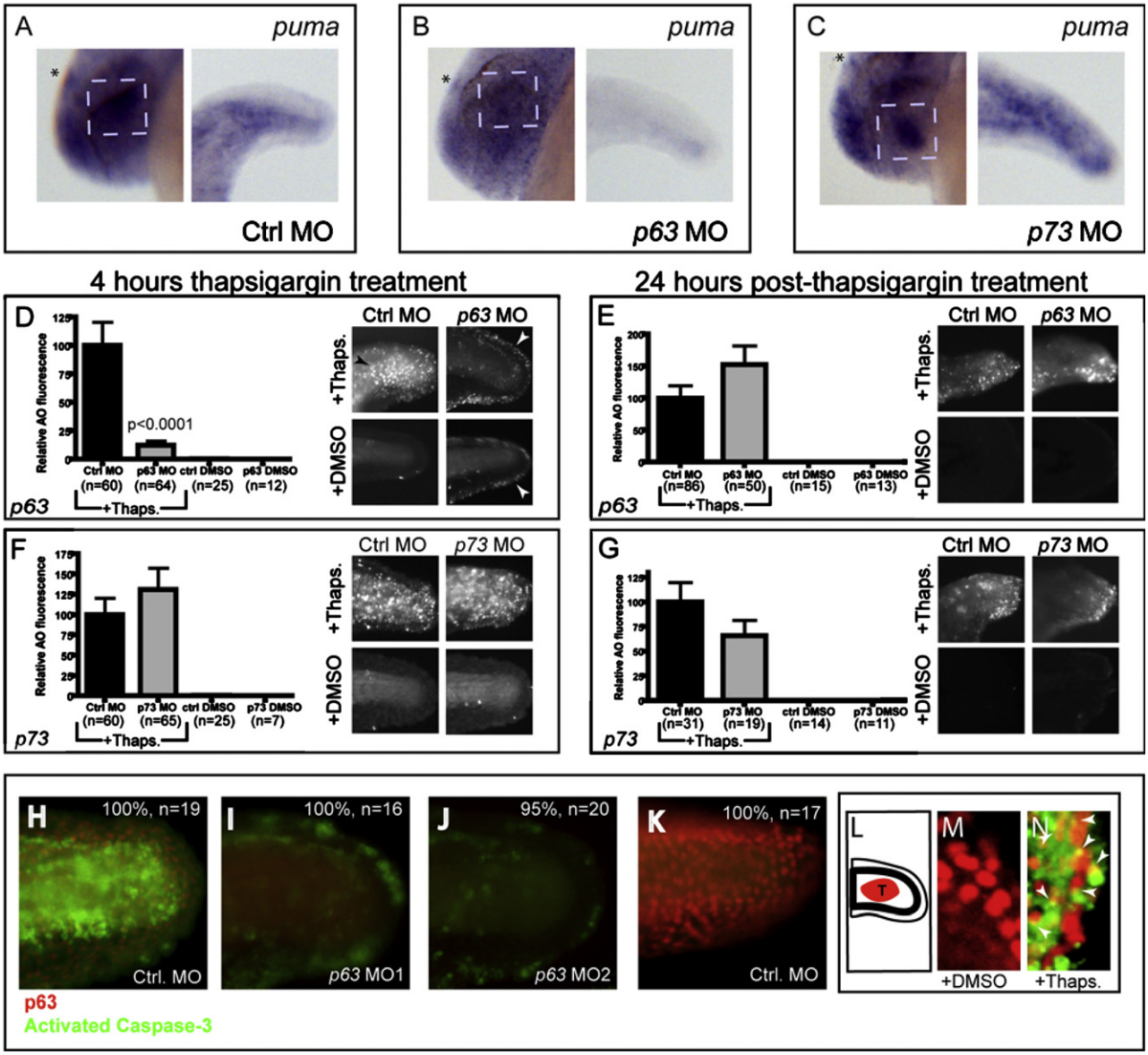

Figure 5. p63, but Not p73, Is Required for ER Stress-Induced *puma* Expression and 4 Hr Apoptosis

(A and B) Compared to thapsigargin-treated control morphants (100% with high *puma* expression, n = 16) thapsigargin-treated *p63* morphants had reduced *puma* expression in the epiphysis, lens, and tail (78% with reduced expression, n = 18).

(C) Thapsigargin-treated p73 morphants had similar *puma* expression (94%, n = 18) compared to control morphants. Asterisk, epiphysis; dashed box, lens.

(D and E) *p63* and control morphants were assayed for apoptosis by AO staining at 4 hr after thapsigargin or DMSO treatment, or (E) washed out and assayed by AO staining 24 hr later. See also Figure S4 and Figure S5. In (D), note the weak AO staining in the outer fin epidermis (white arrowheads) of *p63* morphants, regardless of thapsigargin treatment, but the nearly complete block of cell death in the lateral epidermis compared to the same region in thapsigargin-treated control morphants (black arrowhead).

(F and G) *p73* morphants were processed the same as for *p63* morphants. *p73* morpholino injection does not block either (F) 4 hr thapsigargin-induced apoptosis or (G) 28 hr thapsigargin-induced apoptosis.

(H–J) Embryos were injected with either (H) control morpholino, (I) p63 MO1 or (J) p63 MO2, then treated with thapsigargin for 4 hr and assayed for p63 expression (red) and activated Caspase-3 (green) by immunofluorescence microscopy. Note the severe reduction in p63 and Caspase-3 expression in both p63 morphants (I and J) compared to control morphants (H).

(K) Control embryos treated with DMSO showed extensive p63 expression with minimal Caspase-3 positivity.

(L–N) Confocal analysis of coimmunofluorescence in embryos treated with DMSO (M) or thapsigargin (N) to analyze p63 expression (red) and activated Caspase-3 (green). Note the extensive colocalization of activated Caspase-3 with p63 in (N), marked with arrowheads. (L) A schematic representation of the imaged region in (M) and (N). All graphical data are represented as means ± SEM.

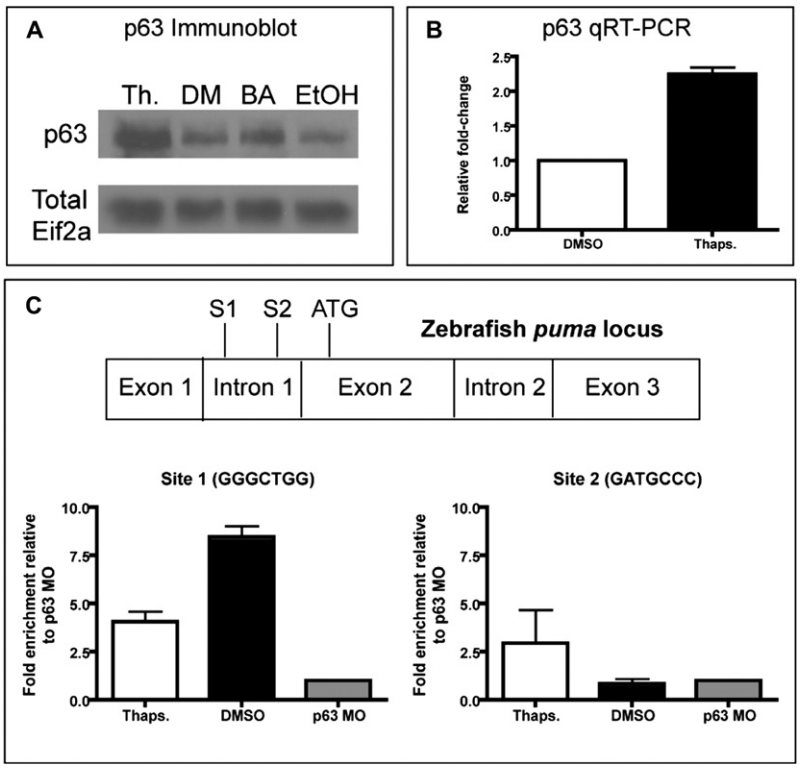

Figure 6. p63 Is Transcriptionally Increased and Directly Binds the *puma* Promoter

(A) Western blot to analyze p63 protein levels following 4 hr of thapsigargin (Th.) treatment, DMSO (DM) treatment, Brefeldin A (BA) treatment, or Ethanol (EtOH) treatment. Note the increased levels of p63 following both thapsigargin and brefeldin A treatment relative to their respective vehicle-only controls. Total Eif2-α antibody was used to control for loading.

(B) p63 qRT-PCR revealed an increase in p63 transcript levels following 3 hr of thapsigargin treatment relative to controls (the sum of three experiments is represented).

(C) Chromatin Immunoprecipitation to determine p63 binding to the puma promoter. Data are representative of experiments from two sets of biological samples, and are normalized to the p63 morpholino-injected negative control sample (p63 MO).

the tail epidermis, p63 mediates a 4 hr ER stress-induced apoptotic response via transcriptional activation of *puma*.

p63 Is Activated by ER Stress and Directly Binds to the *puma* Promoter

Given the link between p63 and the apoptotic response of epithelial cells to ER stress, we sought to elucidate the mechanism(s) underlying p63 activation and its role in the ER stress response. One major mechanism for p63 activation in other systems is an increase in protein levels, either through increased *p63* transcription or stabilization of the p63 protein (Antonini et al., 2006; Rossi et al., 2006a, 2006b). We initially examined whether p63 protein levels were increased by performing immunoblotting for p63 from pooled thapsigargin-treated *p53* mutant embryos compared to DMSO controls. We noted an increase of p63 protein levels in thapsigargin-treated embryos, indicating that p63 levels rise in response to ER stress (Figure 6A). To confirm that this effect was not specific to thapsigargin, we also compared brefeldin A-treated with ethanol-treated control lysates, observing an increase in p63 levels after treatment with brefeldin A (Figure 6A) that was not as robust as for thapsigargin treatment, consistent with the somewhat lower levels of epidermal apoptosis triggered by this drug. To test whether p63 was increased transcriptionally, we performed qRT-PCR on pooled thapsigargin-treated embryos compared to DMSO controls (Figure 6B). This led to an ~2-fold increase in p63 transcript levels, consistent with our western blotting results. Thus, when ER stress activates *p63* transcription, the resultant in p63 protein levels likely contributes to the activation of *puma* and subsequent apoptosis in the epidermis.

To determine whether p63 binds directly to the *puma* promoter following ER stress to activate gene transcription, we performed chromatin immunoprecipitation (ChIP) from thapsigargin and DMSO-treated control embryos using an anti-p63 antibody (Figure 5C). The zebrafish *puma* locus contains two conserved p53 response elements in the first intron (www.ensembl.org), similar to mouse and human *puma* (Wu et al., 2005), leading us to ask whether p63 binds to these response elements in vivo during thapsigargin-induced ER stress. As a negative control for this experiment, we used *p63* morphant embryos, which express much lower levels of p63 protein (Figures 5H–5K). After measuring the fold enrichment in immunoprecipitated chromatin compared to input chromatin by qPCR and normalizing the result to the fold-enrichment in our p63 morphant sample, we found that p63 constitutively binds Site 1 (GGGCTGG) within the *puma* first intron (Figure 6C). The fold-enrichment was higher in DMSO samples than in thapsigargin-treated samples (~8-fold versus ~4-fold), indicating that p63 binding to this site cannot explain the ER-stress induced increase in puma expression. Importantly, we observed enrichment of the levels of p63 binding to Site 2 (GATGCCC) in the thapsigargin-treated sample (~2.5-fold), but not in the DMSO control sample (Figure 5C). Thus, our ChIP results show that Site 1 in the *puma* first intron is constitutively bound by p63, while Site 2 is bound only upon thapsigargin treatment, and thus is likely involved in the p63-mediated transcriptional upregulation of *puma* during the ER stress response.

Connexin 31 Mutants Trigger ER Stress-Induced Apoptosis through p63

To investigate the clinical relevance of the epidermal p63-ER stress pathway, we generated a zebrafish model of human erythrokeratoderma variabilis (EKV). This hereditary disease of the skin epidermis, characterized by hyperkeratosis and erythema, is caused by mutations in the hemichannel protein Connexin 31 (Cx31) (Hunzeker et al., 2008). Recently, the Cx31 mutation C86S, a dominantly inherited mutation leading to the human disease, was shown to trigger apoptosis in cultured epidermal

cells through defective intracellular trafficking and ER stress, rather than through impaired hemichannel function (Tattersall et al., 2009). To determine whether we could model this response in vivo in the zebrafish and whether p63 is required for the apoptotic response, we generated heat-shock inducible constructs containing human Cx31 mutant and wild-type cDNAs fused to EGFP and flanked by *tol2* transposable element sites (Figure 7A). Since coinjection of *tol2* mRNA yields high levels of plasmid integration and low levels of mosaicism (Kawakami, 2007), we injected the wild-type or C86S mutant Cx31 constructs with *tol2* into fertilized eggs of homozygous *p53* mutant embryos at the one-cell stage. We then heat-shocked the embryos at 24 hpf to induce expression of the Cx31-EGFP coding sequences within each of the two constructs. As shown in Figures S6A–S6D, heat-shock for 30 min triggered nearly ubiquitous expression of the Cx31-EGFP constructs throughout the embryos within 2 hr. We next assessed the phenotypes resulting from expression of the Cx31-EGFP constructs, observing a severe phenotype in (C86S)Cx31-EGFP embryos, characterized by disruption of the skin epidermis in 85% of the embryos ($n = 20$) by 3 hr post heat-shock, suggesting induction of an apoptotic response. This phenotype resembles the one obtained in vitro that is thought to contribute to human EKV disease (Tattersall et al., 2009).

Next, we reduced the level of expression by limiting the time of heat shock to 10 min, and injected specific cells into the embryos at the 2- to 4-cell stage to produce mosaic expression. This allowed us to observe the fates of subsets of skin epidermal cells that expressed the Cx31-EGFP constructs (Figure 7A). To measure the level of apoptosis induced by (C86S)Cx31-EGFP expression, we injected this construct or the control (WT)Cx31-EGFP construct and subjected the embryos to heat shock for 10 min at 24 hpf. Using dual immunofluorescence to detect EGFP (green) and activated Caspase-3 (red), and phalloidin (blue) to mark the epidermal cell boundaries (Figures 7B–7E), we found that ~25% of the (C86S)Cx31-EGFP-positive cells underwent apoptosis, compared to ~10% of the (WT)Cx31-EGFP positive cells ($p = 0.0002$) (Figure 7F). As shown by a representative image in Figure 7E, knockdown of *p63* transcripts blocked the epidermal apoptosis caused by the (C86S)Cx31-EGFP mutant construct. Quantitatively, that was a nearly complete loss of the apoptotic cells with each of the p63 MOs (Figure 7F; $p < 0.0001$). These results support the role of ER stress- induced apoptotic cell death in the pathogenesis of human EKV and indicate that this response occurs through the p63-mediated, p53-independent apoptotic axis identified in this study.

DISCUSSION

We have shown that ER stress pathways are activated within 1 hr of thapsigargin treatment in the tail epidermis of 24-hpf zebrafish embryos. This highly conserved ER stress response triggers 4 hr apoptosis through direct activation of *puma* by p63 in the epidermal cell layer, independently of Chop, p53, and p73. This pathway is activated by the mutant (CS86)Cx31 protein in human EKV disease, likely because mutant Cx31 protein activates the unfolded protein response and induces ER stress in epidermal cells as in mammals.

High Levels of ER Stress in the Developing Epidermis Trigger Rapid p53-Independent Apoptosis

Development of the mammalian epidermis involves ER stress as part of the physiological barrier formation process en route to skin maturation (Celli et al., 2011). Additionally, we and others have observed that *bip* and *xbp*, two markers of ER stress induction, are constitutively expressed in the developing zebrafish epidermis (data not shown). Based on these findings, we propose that the epidermis continuously induces low-level ER stress during early development, owing to the massive amounts of membrane and secreted proteins that are produced to form the epidermal basement membrane (Webb et al., 2007). Another tissue in the developing zebrafish, the hatching gland, also expresses these ER stress markers, and a previous study showed that Xbp loss causes massive ER dysfunction indicative of ER stress (Bennett et al., 2007). We propose that the epidermis, like the lens, epiphysis, and hatching gland, is highly sensitized to ER stress induction, and that this tissue undergoes robust apoptosis after excessive ER stress. Thus, when zebrafish embryos are treated at 24 hpf with pharmacological stressors such as thapsigargin and brefeldin A or genetic stressors such as (C86S)Cx31-EGFP, the epidermis is quickly overloaded with ER stress, leading to the death of epidermal cells via induction of *puma* by the transcription factor p63. Furthermore, this activation is independent of p53, which mediates DNA damage-induced apoptosis in the developing zebrafish spinal cord (Berghmans et al., 2005; Langheinrich et al., 2002; Sidi et al., 2008).

Thapsigargin Is a Robust and Rapid Inducer of ER Stress in the Early Embryo

Our tissue-restricted microarray data allow us to implicate *puma* as the critical factor mediating ER stress-induced epidermal apoptosis. They also underscore the activity of thapsigargin in inducing a robust ER stress response within 3 hr in the tail epidermis. Although the calcium-mediated axis-kinking phenotype caused by thapsigargin is often severe, a previous study of the *accordion* mutant, which has the axis-kinking phenotype, did not describe any overt apoptosis during development (Hirata et al., 2004). This mutant lacks the function of a major muscle-specific calcium ATPase pump, resembling the pharmacological effects of thapsigargin treatment in the muscle. In addition, our results were confirmed with a second drug, brefeldin A, that inhibits transport of proteins from the ER to Golgi through a mechanism independent of calcium flux. Thus, thapsigargin and brefeldin A each appear to induce a specific ER stress response in the epidermis via p63 and *puma* within the 4 hr window of our analysis.

p63 Directly Activates *puma* to Trigger ER Stress-Induced Epidermal Apoptosis

By knocking down the transcripts encoding the p53 homologs p63 and p73, we uncovered a role for p63 in the epidermal ER stress response. After its ER stress-mediated activation, p63 directly binds the promoter of the BH3-only cell death inducer *puma* and activates its transcription. Using chromatin immunoprecipitation from whole zebrafish embryos, we found that p63 binds constitutively to one of its response elements within *puma* intron 1. Following ER stress induction, there was

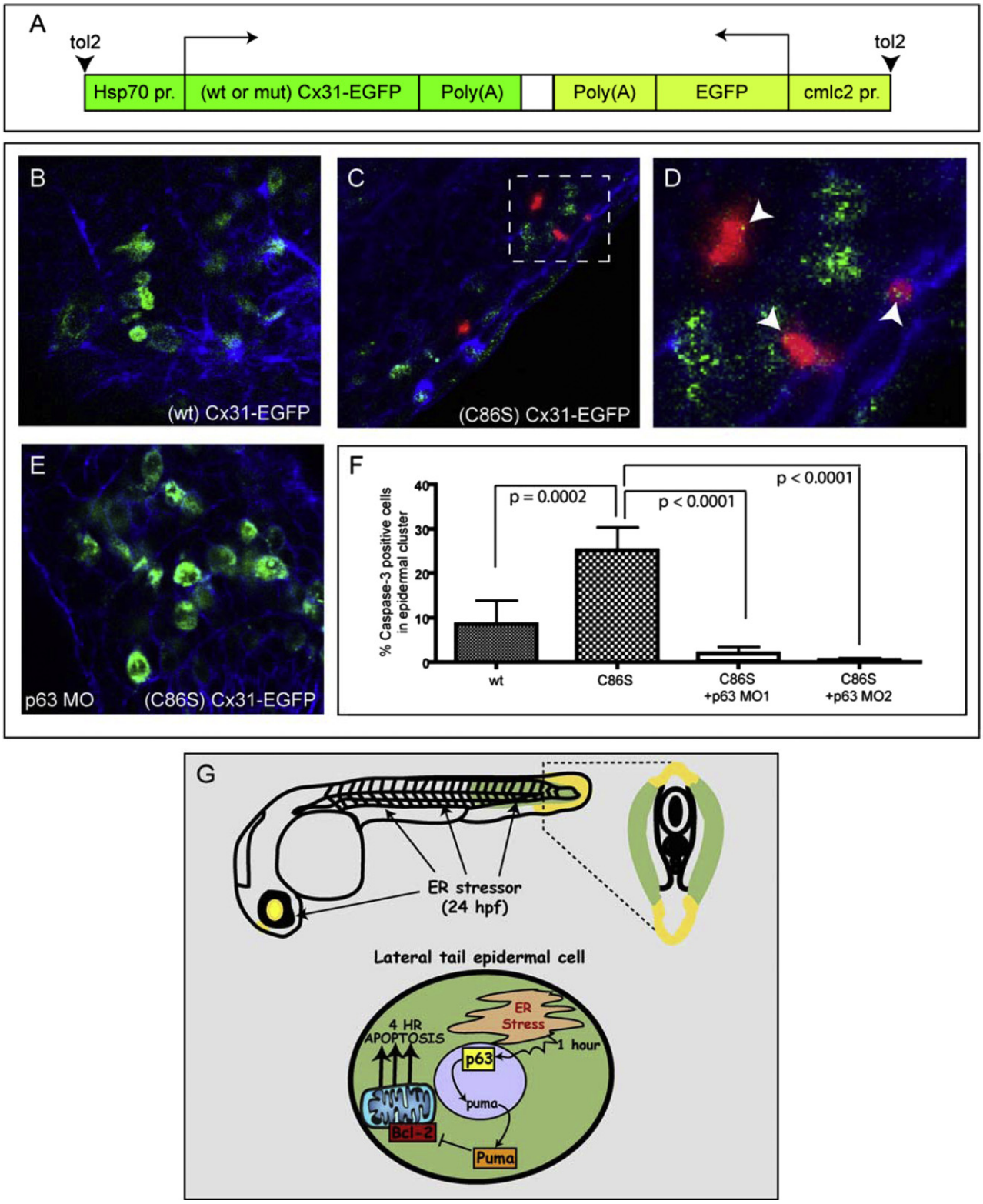

Figure 7. p63 Is Required for Apoptosis Induced by a Mutant Connexin 31 Construct Associated with Human EKV Disease

(A) Overview of the Cx31 DNA constructs used in this study.

(B–F) *p53* mutant embryos were injected with wt or (C86S) mutant Cx31-EGFP constructs, then heat shocked at 24 hpf to induce Cx31-EGFP expression, fixed at 2 hr later, and processed for anti-EGFP (green), anti-activated Caspase-3 (red) and phalloidin staining (blue). See also Figure S6. (B) (wt) Cx31-EGFP caused minimal apoptosis. (C) (C86S) Cx31-EGFP caused a higher level of epidermal apoptosis than (wt) Cx31-EGFP. (D) Zoomed region from (C). (E) Coinjection of p63

increased binding of p63 to a second response element within the same intron, suggesting that this site is responsible for the marked increase in *puma* expression after ER stress. Based on these results and our in situ hybridization data showing that ER stress-induced *puma* expression in the epidermis is markedly diminished after *p63* knockdown, we propose that after ER stress, p63 binds to site 2 within the puma first intron and triggers the expression of this BH3-only gene. Subsequently, cells within the tail epidermis undergo apoptosis, which can be blocked by *Bcl-2* overexpression.

p63 Is Required for Apoptosis Induced by the Human Connexin 31 Mutation C86S

The p63-mediated ER stress pathway we have identified appears to have a role in human disease. The C86S germline mutation in the GJB3 gene, which encodes the Cx31 protein, causes a skin disease called EKV, which is characterized by erythematous patches along with hyperkeratosis. In mammalian keratinocytes, (C86S) Cx31 but not wild-type Cx31, was recently shown to induce cell death through ER stress rather than through disruption of hemichannels at the cell membrane (Tattersall et al., 2009). In addition to the pharmacological induction of ER stress, we show that human Cx31-EGFP with a C86S mutation induces apoptosis in the developing tail epidermis, similar to that observed after treatment with thapsigargin or brefeldin A. By using two different *p63* morpholinos, we show further that the (C86S)Cx31-EGFP construct causes apoptosis in a p63-dependent manner. This implicates the p63-dependent apoptotic axis in the pathogenesis of EKV, where it presumably contributes to the erythema and hyperproliferation of the skin epidermis characteristic of this disease.

EXPERIMENTAL PROCEDURES

Thapsigargin Treatment

Thapsigargin (10 mM, Sigma, St. Louis, MO) in DMSO was diluted 1:20 in E3 egg water, and 10 μl was then added to 1 ml of egg water in a single well of a 12-well tissue culture plate (BD Falcon, Canaan, CT) to make a 5 μM final concentration. A total of 20–25 embryos, no older than 24 hpf at the start of the experiment, were placed in each well. For rapid apoptosis induction, embryos were left for 4 hr in the dark at 28.5°C and processed for either Acridine Orange staining, TUNEL staining, or anti-activated Caspase-3 immunohistochemistry. For the induction of late apoptosis, embryos were left in thapsigargin for 4 hr in the dark at 28.5°, washed three times with E3 egg medium, and replaced at 28.5° for 24 hr. Cell death was then assayed by AO staining.

Apoptosis Quantitation with Volocity Software

To quantify AO or TUNEL positivity in the tail, we mounted stained embryos laterally in 0.8% low melting point agarose within 60 × 15 mm Petri dishes (Falcon). Subsequently, stained embryos were visualized by fluorescent microscopy with a Nikon SMZ1500 zoom stereomicroscope (Nikon Instruments, Melville, NY) using a 488 nm filter for the green fluorescent signal; photographs were taken with a Nikon Digital Sight DS-2MBWc black and white camera with NIS Elements software. All images were acquired at the same magnification, exposure, and gain. Subsequently, acquired images were rotated and cropped to a 3" × 3" square extending from the tip of the tail anteriorly using Adobe Photoshop software. Only images in focus were used for Volocity analysis, in which fluorescence intensity was calculated by first setting the threshold intensity above background in a representative control morpholino-injected embryo treated with thapsigargin. This was done for each experiment, since the threshold varied between experiments. Next, the total fluorescence intensity at or above the threshold value was calculated for each image. Means were calculated for each treatment using Prism software, and Microsoft Excel software was used to convert all data points to a percentage of the control mean. Unless otherwise noted, three independent experiments were conducted for each morpholino injection and were summed for graphical illustration and statistical analysis in Prism. Unpaired Student's t tests were performed in Prism to determine the p value for each treatment compared to controls. All findings are reported as means ± SEM.

Chromatin Immunoprecipitation

For each sample (Ctrl MO + DMSO, Ctrl MO + Thapsigargin, p63 MO1 + Thapsigargin), input chromatin was saved following sonication to determine enrichment. Chromatin immunoprecipitation was performed using Dynabeads as described on the ZFIN website for whole zebrafish embryos (https://wiki.zfin.org/display/prot/Chromatin+Immunoprecipitation+%28ChIP%29+Protocol+using+Dynabeads). 4A4 anti-human p63 antibody (Santa Cruz) was used for immunoprecipitation. The sequences for the primers used for subsequent qPCR of the *puma* promoter and additional information can be found in the Supplemental Experimental Procedures.

Microarrays

Tails from 20 embryos in each experimental condition were dissected and processed using Trizol (Ambion) to extract RNA. Three biological samples on separate days were generated and submitted simultaneously to the DFCI Microarray Core Facility for processing. GeneChip Zebrafish Genome Array chips (Affymetrix) were used for hybridization, representing ~14,900 transcripts. Subsequently, data processing was performed using dChip software (Cheng Li laboratory, DFCI) to generate a list of transcripts with p values <0.05 and fold-change of >1.5 per sample for AB + Thapsigargin versus AB + DMSO RNAs. This list of genes was then sorted in descending order of fold change and fold-change values for the same gene list were included from *p53* mutant samples (Thapsigargin versus DMSO-treated). The top 50 upregulated genes following thapsigargin treatment were used to generate a heatmap in GenePattern (Broad Institute).

Caspase-3/Connexin 31-EGFP Immunofluorescence and Confocal Microscopy

Heat-shocked embryos were fixed for 1 hr in 4% paraformaldehyde at room temperature, then washed into PBST and permeabilized in PBS + 0.1% Triton for 30 min at room temperature. Embryos were blocked in 2% FBS/PBST for 1 hr, and then incubated in primary antibody overnight at 4°C. The anti-activated Caspase-3 antibody was used at a dilution of 1:200, anti-EGFP at 1:500. For Caspase-3 detection, an Alexa 647 goat anti-rabbit secondary antibody was used, while for EGFP detection, an Alexa 488 goat anti-mouse secondary antibody was used. Subsequently, embryos were washed in PBST and stained in phalloidin for 1 hr prior to imaging. Imaging was performed using a Leica SP5 confocal microscope with a 20× water immersion lens. Counts were performed in clusters of EGFP positive and EGFP/Caspase 3 positive cells between the yolk extension and the end of the tail.

SUPPLEMENTAL INFORMATION

Supplemental Information includes Supplemental Experimental Procedures and six figures and can be found with this article online at doi:10.1016/j.devcel.2011.07.012.

MO1 blocked the apoptosis induced by (C86S) Cx31-EGFP. (F) Quantification of apoptosis expressed as % Caspase-3 positive cells in an EGFP positive epidermal cluster. At least eight embryos per condition were used for quantitation.
(G) A model for the mechanism of ER stress-induced apoptosis in the developing epidermis.

ACKNOWLEDGMENTS

We thank John Gilbert, Elspeth Payne, and Samuel Sidi for critical readings of the manuscript. Confocal microscopy images for this study were acquired in the Confocal and Light Microscopy Core Facility at the Dana-Farber Cancer Institute with the assistance of Lisa Cameron. U.J.P. was supported by the Alex's Lemonade Stand Foundation Young Investigator Award, U.J.P. and S.C. by NIH 3R01CA119066-04S1, and A.T.L. by NIH R01CA119066.

Received: April 23, 2010
Revised: April 12, 2011
Accepted: July 22, 2011
Published online: September 12, 2011

REFERENCES

Abrams, J.M., White, K., Fessler, L.I., and Steller, H. (1993). Programmed cell death during Drosophila embryogenesis. Development *117*, 29–43.

Antonini, D., Rossi, B., Han, R., Minichiello, A., Di Palma, T., Corrado, M., Banfi, S., Zannini, M., Brissette, J.L., and Missero, C. (2006). An autoregulatory loop directs the tissue-specific expression of p63 through a long-range evolutionarily conserved enhancer. Mol. Cell. Biol. *26*, 3308–3318.

Bakkers, J., Hild, M., Kramer, C., Furutani-Seiki, M., and Hammerschmidt, M. (2002). Zebrafish DeltaNp63 is a direct target of Bmp signaling and encodes a transcriptional repressor blocking neural specification in the ventral ectoderm. Dev. Cell *2*, 617–627.

Bennett, J.T., Joubin, K., Cheng, S., Aanstad, P., Herwig, R., Clark, M., Lehrach, H., and Schier, A.F. (2007). Nodal signaling activates differentiation genes during zebrafish gastrulation. Dev. Biol. *304*, 525–540.

Berghmans, S., Murphey, R.D., Wienholds, E., Neuberg, D., Kutok, J.L., Fletcher, C.D., Morris, J.P., Liu, T.X., Schulte-Merker, S., Kanki, J.P., et al. (2005). tp53 mutant zebrafish develop malignant peripheral nerve sheath tumors. Proc. Natl. Acad. Sci. USA *102*, 407–412.

Bertolotti, A., Zhang, Y., Hendershot, L.M., Harding, H.P., and Ron, D. (2000). Dynamic interaction of BiP and ER stress transducers in the unfolded-protein response. Nat. Cell Biol. *2*, 326–332.

Calfon, M., Zeng, H., Urano, F., Till, J.H., Hubbard, S.R., Harding, H.P., Clark, S.G., and Ron, D. (2002). IRE1 couples endoplasmic reticulum load to secretory capacity by processing the XBP-1 mRNA. Nature *415*, 92–96.

Celli, A., Mackenzie, D.S., Crumrine, D.S., Tu, C.L., Hupe, M., Bikle, D.D., Elias, P.M., and Mauro, T.M. (2011). Endoplasmic reticulum Ca(2+) depletion activates XBP1 and controls terminal differentiation in keratinocytes and epidermis. Br. J. Dermatol. *164*, 16–25.

Cox, J.S., Shamu, C.E., and Walter, P. (1993). Transcriptional induction of genes encoding endoplasmic reticulum resident proteins requires a transmembrane protein kinase. Cell *73*, 1197–1206.

Fribley, A., Zhang, K., and Kaufman, R.J. (2009). Regulation of apoptosis by the unfolded protein response. Methods Mol. Biol. *559*, 191–204.

Galehdar, Z., Swan, P., Fuerth, B., Callaghan, S.M., Park, D.S., and Cregan, S.P. (2010). Neuronal apoptosis induced by endoplasmic reticulum stress is regulated by ATF4-CHOP-mediated induction of the Bcl-2 homology 3-only member PUMA. J. Neurosci. *30*, 16938–16948.

Harding, H.P., Novoa, I., Zhang, Y., Zeng, H., Wek, R., Schapira, M., and Ron, D. (2000). Regulated translation initiation controls stress-induced gene expression in mammalian cells. Mol. Cell *6*, 1099–1108.

Harding, H.P., Zhang, Y., and Ron, D. (1999). Protein translation and folding are coupled by an endoplasmic-reticulum-resident kinase. Nature *397*, 271–274.

Harms, K., Nozell, S., and Chen, X. (2004). The common and distinct target genes of the p53 family transcription factors. Cell. Mol. Life Sci. *61*, 822–842.

Haze, K., Yoshida, H., Yanagi, H., Yura, T., and Mori, K. (1999). Mammalian transcription factor ATF6 is synthesized as a transmembrane protein and activated by proteolysis in response to endoplasmic reticulum stress. Mol. Biol. Cell *10*, 3787–3799.

Hirata, H., Saint-Amant, L., Waterbury, J., Cui, W., Zhou, W., Li, Q., Goldman, D., Granato, M., and Kuwada, J.Y. (2004). accordion, a zebrafish behavioral mutant, has a muscle relaxation defect due to a mutation in the ATPase Ca2+ pump SERCA1. Development *131*, 5457–5468.

Hunzeker, C.M., Soldano, A.C., and Levis, W.R. (2008). Erythrokeratoderma variabilis. Dermatol. Online J. *14*, 13.

Jette, C.A., Flanagan, A.M., Ryan, J., Pyati, U.J., Carbonneau, S., Stewart, R.A., Langenau, D.M., Look, A.T., and Letai, A. (2008). BIM and other BCL-2 family proteins exhibit cross-species conservation of function between zebrafish and mammals. Cell Death Differ. *15*, 1063–1072.

Kamada, S., Kikkawa, U., Tsujimoto, Y., and Hunter, T. (2005). Nuclear translocation of caspase-3 is dependent on its proteolytic activation and recognition of a substrate-like protein(s). J. Biol. Chem. *280*, 857–860.

Kawakami, K. (2007). Tol2: a versatile gene transfer vector in vertebrates. Genome Biol. *8* (*Suppl 1*), S7.

Kopito, R.R. (1997). ER quality control: the cytoplasmic connection. Cell *88*, 427–430.

Langheinrich, U., Hennen, E., Stott, G., and Vacun, G. (2002). Zebrafish as a model organism for the identification and characterization of drugs and genes affecting p53 signaling. Curr. Biol. *12*, 2023–2028.

Lee, H., and Kimelman, D. (2002). A dominant-negative form of p63 is required for epidermal proliferation in zebrafish. Dev. Cell *2*, 607–616.

Lin, J.H., Walter, P., and Yen, T.S. (2008). Endoplasmic reticulum stress in disease pathogenesis. Annu. Rev. Pathol. *3*, 399–425.

Malhotra, J.D., and Kaufman, R.J. (2007). The endoplasmic reticulum and the unfolded protein response. Semin. Cell Dev. Biol. *18*, 716–731.

Matsumoto, M., Minami, M., Takeda, K., Sakao, Y., and Akira, S. (1996). Ectopic expression of CHOP (GADD153) induces apoptosis in M1 myeloblastic leukemia cells. FEBS Lett. *395*, 143–147.

Maytin, E.V., Ubeda, M., Lin, J.C., and Habener, J.F. (2001). Stress-inducible transcription factor CHOP/gadd153 induces apoptosis in mammalian cells via p38 kinase-dependent and -independent mechanisms. Exp. Cell Res. *267*, 193–204.

Mori, K., Ma, W., Gething, M.J., and Sambrook, J. (1993). A transmembrane protein with a cdc2+/CDC28-related kinase activity is required for signaling from the ER to the nucleus. Cell *74*, 743–756.

Okamura, K., Kimata, Y., Higashio, H., Tsuru, A., and Kohno, K. (2000). Dissociation of Kar2p/BiP from an ER sensory molecule, Ire1p, triggers the unfolded protein response in yeast. Biochem. Biophys. Res. Commun. *279*, 445–450.

Pahl, H.L., and Baeuerle, P.A. (1995). A novel signal transduction pathway from the endoplasmic reticulum to the nucleus is mediated by transcription factor NF-kappa B. EMBO J. *14*, 2580–2588.

Pietsch, E.C., Sykes, S.M., McMahon, S.B., and Murphy, M.E. (2008). The p53 family and programmed cell death. Oncogene *27*, 6507–6521.

Puthalakath, H., O'Reilly, L.A., Gunn, P., Lee, L., Kelly, P.N., Huntington, N.D., Hughes, P.D., Michalak, E.M., McKimm-Breschkin, J., Motoyama, N., et al. (2007). ER stress triggers apoptosis by activating BH3-only protein Bim. Cell *129*, 1337–1349.

Pyati, U.J., Look, A.T., and Hammerschmidt, M. (2007). Zebrafish as a powerful vertebrate model system for in vivo studies of cell death. Semin. Cancer Biol. *17*, 154–165.

Rao, R.V., Ellerby, H.M., and Bredesen, D.E. (2004). Coupling endoplasmic reticulum stress to the cell death program. Cell Death Differ. *11*, 372–380.

Reimertz, C., Kögel, D., Rami, A., Chittenden, T., and Prehn, J.H. (2003). Gene expression during ER stress-induced apoptosis in neurons: induction of the BH3-only protein Bbc3/PUMA and activation of the mitochondrial apoptosis pathway. J. Cell Biol. *162*, 587–597.

Rentzsch, F., Kramer, C., and Hammerschmidt, M. (2003). Specific and conserved roles of TAp73 during zebrafish development. Gene *323*, 19–30.

Robu, M.E., Larson, J.D., Nasevicius, A., Beiraghi, S., Brenner, C., Farber, S.A., and Ekker, S.C. (2007). p53 activation by knockdown technologies. PLoS Genet. *3*, e78.

Ron, D., and Walter, P. (2007). Signal integration in the endoplasmic reticulum unfolded protein response. Nat. Rev. Mol. Cell Biol. *8*, 519–529.

Rossi, M., Aqeilan, R.I., Neale, M., Candi, E., Salomoni, P., Knight, R.A., Croce, C.M., and Melino, G. (2006a). The E3 ubiquitin ligase Itch controls the protein stability of p63. Proc. Natl. Acad. Sci. USA *103*, 12753–12758.

Rossi, M., De Simone, M., Pollice, A., Santoro, R., La Mantia, G., Guerrini, L., and Calabrò, V. (2006b). Itch/AIP4 associates with and promotes p63 protein degradation. Cell Cycle *5*, 1816–1822.

Samali, A., Fitzgerald, U., Deegan, S., and Gupta, S. (2010). Methods for monitoring endoplasmic reticulum stress and the unfolded protein response. Int. J. Cell Biol. *2010*, 830307.

Sidi, S., Sanda, T., Kennedy, R.D., Hagen, A.T., Jette, C.A., Hoffmans, R., Pascual, J., Imamura, S., Kishi, S., Amatruda, J.F., et al. (2008). Chk1 suppresses a caspase-2 apoptotic response to DNA damage that bypasses p53, Bcl-2, and caspase-3. Cell *133*, 864–877.

Sidrauski, C., and Walter, P. (1997). The transmembrane kinase Ire1p is a site-specific endonuclease that initiates mRNA splicing in the unfolded protein response. Cell *90*, 1031–1039.

Tattersall, D., Scott, C.A., Gray, C., Zicha, D., and Kelsell, D.P. (2009). EKV mutant connexin 31 associated cell death is mediated by ER stress. Hum. Mol. Genet. *18*, 4734–4745.

Travers, K.J., Patil, C.K., Wodicka, L., Lockhart, D.J., Weissman, J.S., and Walter, P. (2000). Functional and genomic analyses reveal an essential coordination between the unfolded protein response and ER-associated degradation. Cell *101*, 249–258.

Webb, A.E., and Kimelman, D. (2005). Analysis of early epidermal development in zebrafish. Methods Mol. Biol. *289*, 137–146.

Webb, A.E., Sanderford, J., Frank, D., Talbot, W.S., Driever, W., and Kimelman, D. (2007). Laminin alpha5 is essential for the formation of the zebrafish fins. Dev. Biol. *311*, 369–382.

Wu, W.S., Heinrichs, S., Xu, D., Garrison, S.P., Zambetti, G.P., Adams, J.M., and Look, A.T. (2005). Slug antagonizes p53-mediated apoptosis of hematopoietic progenitors by repressing puma. Cell *123*, 641–653.

Yang, A., Kaghad, M., Wang, Y., Gillett, E., Fleming, M.D., Dötsch, V., Andrews, N.C., Caput, D., and McKeon, F. (1998). p63, a p53 homolog at 3q27-29, encodes multiple products with transactivating, death-inducing, and dominant-negative activities. Mol. Cell *2*, 305–316.

Yoshida, H., Matsui, T., Yamamoto, A., Okada, T., and Mori, K. (2001). XBP1 mRNA is induced by ATF6 and spliced by IRE1 in response to ER stress to produce a highly active transcription factor. Cell *107*, 881–891.

Zinszner, H., Kuroda, M., Wang, X., Batchvarova, N., Lightfoot, R.T., Remotti, H., Stevens, J.L., and Ron, D. (1998). CHOP is implicated in programmed cell death in response to impaired function of the endoplasmic reticulum. Genes Dev. *12*, 982–995.